Peer-reviewed version available at Biomolecules 2019, 9, 728; doi:10.3390/biom9110728

Article

A Dynamic Core in Human NQO1 Controls the Functional and Stability Effects of Ligand Binding and Their Communication across the Enzyme Dimer

Pavla Vankova[1,2], Eduardo Salido [3], David J. Timson[4], Petr Man[1,*] and Angel L. Pey [5,*]

[1] Institute of Microbiology, Academy of Sciences of the Czech Republic, Videnska 1083, Prague 4, 142 20, Czech Republic. pavla.vankova@biomed.cas.cz (P.V.); pman@biomed.cas.cz (P.M.)
[2] Department of Biochemistry, Faculty of Science, Charles University, Hlavova 2030/8, Prague 2, 128 43, Czech Republic; pavla.vankova@biomed.cas.cz (P.V.).
[3] Center for Rare Diseases (CIBERER), Hospital Universitario de Canarias, Universidad de La Laguna, 38320, Tenerife, Spain; edsalido@gmail.com (E.S.).
[4] School of Pharmacy and Biomolecular Sciences, University of Brighton, Huxley Building, Lewes Road, Brighton, BN2 4GJ, Brighton, UK; D.Timson@brighton.ac.uk (D.J.T.)
[5] Department of Physical Chemistry and Unit of Excellence in Chemistry, University of Granada, Av. Fuentenueva s/n, E-18071, Granada, Spain; angelpey@ugr.es (A.L.P).

* Correspondence: pman@biomed.cas.cz (P.M.) or angelpey@ugr.es (A.L.P.).

Abstract: Human NAD(P)H:quinone oxidoreductase 1 (NQO1) is a multi-functional protein whose alteration is associated with cancer, Parkinson´s and Alzheimer´s diseases. NQO1 displays a remarkable functional chemistry, capable of binding different functional ligands that modulate its activity, stability and interaction with proteins and nucleic acids. Our understanding on this functional chemistry is limited by the difficulty of obtaining structural and dynamic information on many of these states. Herein, we have used hydrogen/deuterium exchange monitored by mass-spectrometry (HDXMS) to investigate the structural dynamics of NQO1 in three ligation states: without ligands ($NQO1_{apo}$), with FAD ($NQO1_{holo}$) and with FAD and the inhibitor dicoumarol ($NQO1_{dic}$). We show that $NQO1_{apo}$ has a minimally stable folded core holding the protein dimer and with FAD and dicoumarol ligand binding sites populating binding non-competent conformations. Binding of FAD significantly decreases protein dynamics and stabilizes the FAD and dicoumarol binding sites as well as the monomer:monomer interface. Dicoumarol binding further stabilizes all three functional sites, a result not previously anticipated by available crystallographic models. Our work provides an experimental perspective into the communication of stability effects through the NQO1 dimer, valuable to understand at the molecular level the effects of disease-associated variants, post-translation modifications and ligand binding cooperativity in NQO1.

Keywords: Protein structural dynamics; NQO1; ligand binding; protein stability; Allostery; Protein degradation.

1. Introduction

Human NAD(P)H:quinone oxidoreductase 1 (NQO1; EC 1.6.5.2) is a multifunctional stress protein mostly localized in the cellular cytosol [1]. NQO1 expression is upregulated as a response to different types of cellular stress and through several mechanisms, including the antioxidant response through Nrf2-mediated and Ah2 signaling pathways [1, 2, 3, 4].

NQO1 displays multiple enzymatic and non-enzymatic functions [1, 2, 3, 4, 5]. NQO1 catalyses different reactions with cytoprotective and metabolic roles such as the two electron reduction of quinones to form hydroquinones [2, 6], reduction of coenzyme Q_{10} and vitamin E to their antioxidant form [2], scavenging reactive oxygen species [1, 2, 3, 7], reduction of catecholamines and vitamin K [1, 2] and maintenance of the NADH/NAD^+ redox balance [3, 8]. The main features of these biochemical reactions involving NQO1 have been investigated in detail mainly through enzymological and structural analyses. Structurally, the enzyme forms obligate functional homodimers, with two active sites located in the monomer:monomer interface (MMI) and each monomer consists of two different domains: i) an N-terminal domain spanning residues 1-224 that contains part of the active site and it is involved in the tight binding of one FAD molecule per monomer and protein dimerization; ii) a C-terminal domain (residues 225-274) that contributes to stabilize the protein dimer and to the binding of the NAD(P)H coenzyme and the substrates [1, 4, 9, 10, 11, 12, 13, 14]. The functional cycle of NQO1 generally involves two steps according to a *ping-pong* mechanism: first, in the reductive half-reaction, a NAD(P)H molecule binds to the enzyme and rapidly reduces the FAD to $FADH_2$ (with a second-order rate constant of ~10^9 $M^{-1}{\cdot}s^{-1}$) with the subsequent release of the oxidized nicotinamide dinucleotide; and second, in a slower oxidative half-reaction (with a second-order rate constant of ~10^5-10^6 $M^{-1}{\cdot}s^{-1}$), the substrate binds and it is reduced by the $FADH_2$ thus regenerating the flavin in the oxidized form and releasing the reduced product [1, 10]. This catalytic cycle is known to be inhibited by different coumarin-based molecules (the best characterized is the biscoumarin, dicoumarol) that act as competitive inhibitors by blocking the NAD(P)H access to the active site by partially occupying the NAD(P)H binding site [1, 15]. Importantly, comparison of the crystal structures of NQO1 with FAD bound ($NQO1_{holo}$) with that containing also dicoumarol bound ($NQO1_{dic}$) have revealed that inhibitor binding causes only minor structural rearrangements in the conformation that localize at the surface of the catalytic site [15]. Among non-enzymatic functions, we must highlight the ability of NQO1 to develop protein:protein and protein:RNA interactions [1, 2, 16, 17, 18, 19, 20]. In particular, protein:protein interactions involving NQO1 are relevant to understand its multiple roles in physiological and pathological processes. NQO1 interacts with key transcription factors associated with cancer (e.g. p53, p73α and HIF-1α) [17, 18] and proteins involved in HIV infection (e.g. Tat protein) [19], and these interactions increase the intracellular stability of these protein partners by preventing their degradation by the proteasome. These protein:protein interactions presumably depend on the functional state of NQO1: binding of NADH may increase the strength of these interactions while dicoumarol binding has the opposite effect [9, 17, 19]. In addition, $NQO1_{holo}$ binds to the 20S particle of the proteasome and inhibits its proteolytic activity, while FAD withdrawal (i.e. $NQO1_{apo}$) renders NQO1 susceptible to degradation by this mechanism [16].

Alterations in NQO1 stability and function are associated to different extent with a variety of human diseases, including cancer, neurological disorders (such as Parkinson´s and Alzheimer´s disease, multiple sclerosis and schizophrenia) and cardiovascular diseases [1, 21]. In these cases, either the wild-type (WT) NQO1 protein and/or a common polymorphic variant (causing a Pro187Ser amino acid exchange) have been found associated with increased disease predisposition. The Pro187Ser variant decreases the activity due to a large defect in FAD binding (10 to 40-fold lower affinity than that of WT) and in conformational stability leading to its rapid intracellular degradation by the proteasome [1, 10, 14, 16, 22, 23, 24, 25]. In general, reduced NQO1 activity or protein levels are commonly observed under these pathological conditions [1, 26], although for the particular case of cancer, overexpression of NQO1 is also associated with cancer progression which makes pharmacological inhibition of NQO1 (e.g. by dicoumarol or related compounds) an interesting therapeutic strategy to treat this disease [27, 28, 29]. Linked to some of these pathological conditions, the intracellular stability of NQO1 WT is controlled by the population of the $NQO1_{apo}$ state, which is efficiently targeted to the ubiquitin-dependent proteasomal degradation pathway [14, 25, 30]. Recent works also demonstrated that alterations in the phosphorylation pattern of NQO1 WT at different sites might be associated with these pathological states, likely

Peer-reviewed version available at Biomolecules 2019, 9, 728; doi:10.3390/biom9110728

through effects on the FAD binding affinity and consequently on the intracellular stability of NQO1 WT [26, 30, 31].

NQO1 is an excellent model to decipher the role of protein dynamics in the function and stability of flavin-dependent enzymes, the role of ligand binding in disease-associated protein stability and the molecular mechanisms by which mutations cause loss-of-function genetic diseases [1, 5, 9, 10, 14, 25, 30, 32, 33, 34]. FAD binding to NQO1 WT triggers a large conformational change that can be observed by some biophysical techniques (circular dichroism, infrared and NMR spectroscopies or small-angle X-ray scattering) and increases the kinetic stability of the protein dimer, although high resolution structural information is only available for the $NQO1_{holo}$ state [9, 10, 11, 14, 22, 34, 35]. This structural change is accompanied by significant changes in overall protein flexibility (evidence provided by proteolysis experiments and structure-based analyses of FAD binding energetics) [10, 14, 34], presumably linked to the fast degradation of $NQO1_{apo}$ vs. $NQO1_{holo}$ in the cell [14, 25], although no high-resolution experimental information on these dynamic changes is available [14]. Regarding dicoumarol binding, the comparison of the X-ray crystallographic structure of $NQO1_{holo}$ and $NQO1_{dic}$ has revealed only local changes in protein structure at the active site [15] and thus, these did not provide details on the remarkable stabilizing effect of dicoumarol binding on the overall conformational stability and the dynamics of the C-terminal domain [14]. A critical role of protein dynamics in the mechanisms causing alterations in NQO1 function due to the Pro187Ser polymorphism and other rare cancer-associated mutations, phosphorylation at specific sites as well as the effect of suppressor mutations of the Pro187Ser phenotype have been put forward from experimental and computational studies [5, 9, 10, 14, 30, 31, 32, 33, 34, 36]. Thus, they also await high-resolution information on the changes in protein dynamics due to these site-specific changes in different ligation states ($NQO1_{apo}$, $NQO1_{holo}$ and $NQO1_{dic}$).

We report herein a detailed experimental analysis on the structural dynamics of human NQO1 in three functionally relevant ligation states ($NQO1_{apo}$, $NQO1_{holo}$ and $NQO1_{dic}$). Our results uncover the existence of a dynamic network within the NQO1 dimer that readily respond to binding of functional ligands and help to explain their effects on NQO1 function and stability *in vitro* and *in vivo*. Our work also provides an experimental benchmark to understand the allosteric effects of disease-associated variants, post-translational modifications and ligand binding in NQO1.

2. Materials and Methods

2.1. Protein expression and purification

Protein expression and purification was carried out as described [30]. *E. coli* BL21(DE3) cells were transformed with the pET46 Ek/LIC vector containing the cDNA of human NQO1 [22] and grown for 16 h in LBA medium (LB containing 0.1 $mg{\cdot}ml^{-1}$ ampicillin at 37 °C). This culture was diluted 40-fold in fresh LBA and grown at 37 °C for 3 h. Expression was then triggered by the addition of IPTG (isopropyl β-D-1-thiogalactopyranoside) at a final concentration of 0.5 mM. Induced cells were incubated for 6 h at 25 °C, harvested by centrifugation, washed with binding buffer (BB, 20 mM sodium phosphate, 300 mM NaCl and 50 mM imidazole at pH 7.4) and frozen overnight at −80 °C. Then, cells were thawn and resuspended in BB containing 1 mM PMSF (phenylmethylsulfonyl fluoride) and lysed by sonication. Crude extracts were clarified by centrifugation (20 min at 20000 g and 4 °C) and supernatants were loaded into immobilized metal affinity chromatography (IMAC) columns (GE Healthcare) equilibrated in BB. Columns were washed with BB and the protein was eluted with elution buffer (BB containing 500 mM imidazole). The eluate was exchanged to 50 mM K-HEPES (2-[4-(2-hydroxyethyl)piperazin-1-yl]ethanesulfonic acid, potassium salt) pH 7.4 using PD-10 columns (GE Healthcare), centrifuged for 30 min at 20000 g and 4 °C and the UV–visible spectra of the supernatants was registered in a HP8453 UV–Visible spectrophotomer (Agilent). This purified holo-protein containing high levels of FAD bound (70-80% based on the absorbance ratio at 450 nm and 280 nm; see also [30, 33, 36]) was stored at −80 °C upon

flash freezing in liquid N_2. Further purification of the NQO1 dimer was carried out by size-exclusion chromatography using a HiLoad® 16/600 Superdex® 200 prep grade (GE Healthcare) and using 20 mM K-HEPES 200 mM NaCl at pH 7.4 as mobile phase. This purified protein was subsequently used to obtain apo-protein upon treatment with BB containing 2 M urea and 2 M KBr, 1 mM DTT (1,4-dithiothreitol) and 1 mM PMSF at 4 °C and separation of the apo-protein and the FAD released was carried out by IMAC at 4 °C. Apo-proteins were finally exchanged to 50 mM K-HEPES at pH 7.4 using PD-10 columns at 4 °C, concentrated using VIVASPIN 6 30000 MWCO PES devices (Sartorius) and stored at −80 °C after flash freezing in liquid N_2.

Purified proteins were verified by mass spectrometry. The intact mass was analyzed through direct infusion on ESI-FT-ICR MS (Figure S1) showing the protein is expressed intact and lacking the N-terminal Met. The dimeric state of $NQO1_{apo}$ and $NQO1_{holo}$ was verified by native ESI-MS (Figure S2).

2.2. Hydrogen/Deuterium Exchange Mass Spectrometry (HDXMS)

Amide hydrogen/deuterium exchange (HDX) of NQO1 was followed for its apo ($NQO1_{apo}$) and holo ($NQO1_{holo}$) forms and the holo form was also analyzed in the presence of dicoumarol ($NQO1_{dic}$). Prior to the exchange, the $NQO1_{holo}$ and $NQO1_{dic}$ at 20 µM concentration were pre-incubated with 10 molar excess of FAD for 5 min. $NQO1_{dic}$ was then further mixed with 10 molar excess of dicoumarol and incubated for another 5 min. The exchange reaction was initiated by a 10× dilution into a D_2O-based 50 mM K-HEPES, pD 7.4, 1 mM TCEP (tris(2-carboxyethyl)phosphine). The exchange was thus followed at 2 µM protein concentration. Deuterium labelling was quenched by 0.5 M Glycine-HCl, pH 2.3 which was added at 1:1 ratio. The samples were then frozen in liquid N_2. Exchange was followed for 10 s, 30 s, 2 min, 5 min, 20 min, 1 h and 3 h where 10 s, 5 min and 3 h samples were done in replicate. Each sample was quickly thawed and injected onto a cooled LC-system. Here the protein was digested on custom made nepenthesin-2 (Nep-2) and pepsin columns coupled in tandem (each having bed volume of 66 µl) and the resulting peptides were trapped on a VanGuard Pre-column (ACQUITY UPLC BEH C18, 130Å, 1.7 µm, 2.1 mm x 5 mm, Waters, Milford, MA) where they were desalted. Solvent used for digestion and desalting (0.4% formic acid (FA) in water) was pumped by 1260 Infinity II Quaternary pump (Agilent Technologies) at a flow rate of 200 µl·min^{-1}. After three minutes of digestion and desalting, the peptides were separated on an analytical column (ACQUITY UPLC BEH C18, 130 Å, 1.7 µm, 1 mm X 100 mm, Waters) using linear gradient (5-45% B in 7min) followed by a quick step to 99% B lasting 5 min. Solvent A was 0.1% FA / 2% acetonitrile (ACN) in water, B was 0.1% FA / 98% ACN in water. Gradient was delivered by 1290 Infinity II LC System (Agilent Technologies) at a flow of 40 µl·min^{-1}. Digestion, desalting and separation were done at 0 °C and pH 2.3 to minimize deuterium loss. The LC-system was connected directly to an electrospray ionization source of a 15T FT-ICR mass spectrometer (Bruker Daltonics) operating in broad-band MS mode. Data were peak picked and exported using DataAnalysis 5.0 and then processed by in-house developed program Deutex (unpublished). Peptides arising from the digestion were identified through a separate data-dependent LC-MS/MS analyses and database searching by MASCOT algorithm. Fully deuterated samples were prepared and used for back-exchange correction as described previously [37, 38]. Differences in deuteration can be considered as significant if they exceed 3.6% or 0.25 Da (calculated as 3x the average standard deviation).

The optimization of digestion conditions including numerous proteolytical setups showed that serial combination of nepenthesin-2 with pepsin, operated at 200 µl·min^{-1} provided the best results in terms of sequence coverage (98.9%, missing the last three amino acids), number of peptides (140), average peptide length (8.3) and redundancy (4.1) (Figure S3). At this point, it should be also noted that the region between 100 and 110 yielded peptides of considerable hydrophobicity for which the signal intensity/quality was just at the threshold level and thus conclusions derived from their analyses must be made with caution. The redundant peptide set was used to calculate deuteration in

shortest possible segments using the overlapping peptides. These analysis provided more detailed non-redundant information (*high resolution set*). Data in this high-resolution set are mainly described in the manuscript (Figures 1-6, Figures S5 and Table S1), while those using experimental peptides (*low resolution set*) are found in Figures S6-S10 and Table S2. Note that the high resolution set essentially lead to the same key conclusions as the low resolution one but, in principle, the former narrows the region for which HDX kinetics is assessed.

To report data on NQO1 segments from HDX-MS, we did not consider the His-tag and used the native sequence from Met1 to Lys274. Therefore, the numbering used along the manuscript differs from that reported in some crystal structures of NQO1, that did not include Met1 and thus numbered the residues from Val1 to Lys273 (Val2 and Lys274 in the native sequence, respectively).

3. Results and discussion

3.1. A stable folded core in NQO1$_{apo}$ with highly dynamic functional sites

The results of time-dependent HDX kinetics for NQO1$_{apo}$ are shown in Figure 1A. Results are presented as the % of the maximal (theoretical) deuterium incorporation for each segment (%D). Virtually all peptides characterized in this work for NQO1 complied with EX2 behavior (the presence of a tiny contribution from EX1 regime can be detected in a few NQO1 peptides; see Figure S4). In the EX2 mechanism, the intrinsic exchange rate constant (k_{int}) is much lower than the rate constant (k_{cl}) for the conversion between non-exchanging (NE-NH) and exchanging (E-NH) states, according to the Linderstrøm-Lang model:

$$NE\text{–}NH \underset{k_{cl}}{\overset{k_{op}}{\leftrightarrow}} E\text{–}NH \xrightarrow{k_{int}} exchanged\ NH$$

Scheme 1. Linderstrøm-Lang model for HDX kinetics.

Assuming a pure EX2 behavior, the rate constant for exchange of individual backbone amides would be equal to the product of the equilibrium constant between NE-NH and E-NH ($K_{op}=k_{op}/k_{cl}$) and k_{int} [39]. Therefore, for this very simple mechanism (note that the conformational equilibrium is simply two-state and experimental HDX is rarely pure EX2), the experimental rate constant for exchange reflects to some extent the local stability (e.g. due to hydrogen bonding and burial in the structure) of secondary structure.

Overall, the HDX kinetics was very heterogeneous among different protein segments of NQO1$_{apo}$ (Figure 1A). Most of the segments showed fast HDX kinetics (typically exchanging more than 20%D in the seconds-minutes time scales) while only a few peptides showed essentially no exchange after 3 h (%D < 20). Thus, in a first approach, we simply discerned between exchanging and non-exchanging segments considering the %D after 3 h (%D < 20 vs. %D ≥ 20, respectively). The functional implications of this simple analysis were considered regarding those residues in different segments belonging to three functional sites: the FAD binding site (FBS), the dicoumarol binding site (DBS) and the monomer:monomer interface (see Figure 1A), as provided by analysis of an X-ray crystallographic structure (PDB 2F1O [15]). It is worth noting that in this structure, the FBS and DBS are located adjacent in the NQO1 monomer (actually, FAD is structurally part of the DBS), and both sites are close to the MMI (Figure 1B). Importantly, most of the residues that belong to the FBS, DBS and MMI are classified as exchanging in NQO1$_{apo}$ (%D ≥ 20; Figure 1A-B).

Preprints (www.preprints.org) | NOT PEER-REVIEWED | Posted: 24 October 2019 doi:10.20944/preprints201910.0281.v1

Peer-reviewed version available at Biomolecules 2019, 9, 728; doi:10.3390/biom9110728

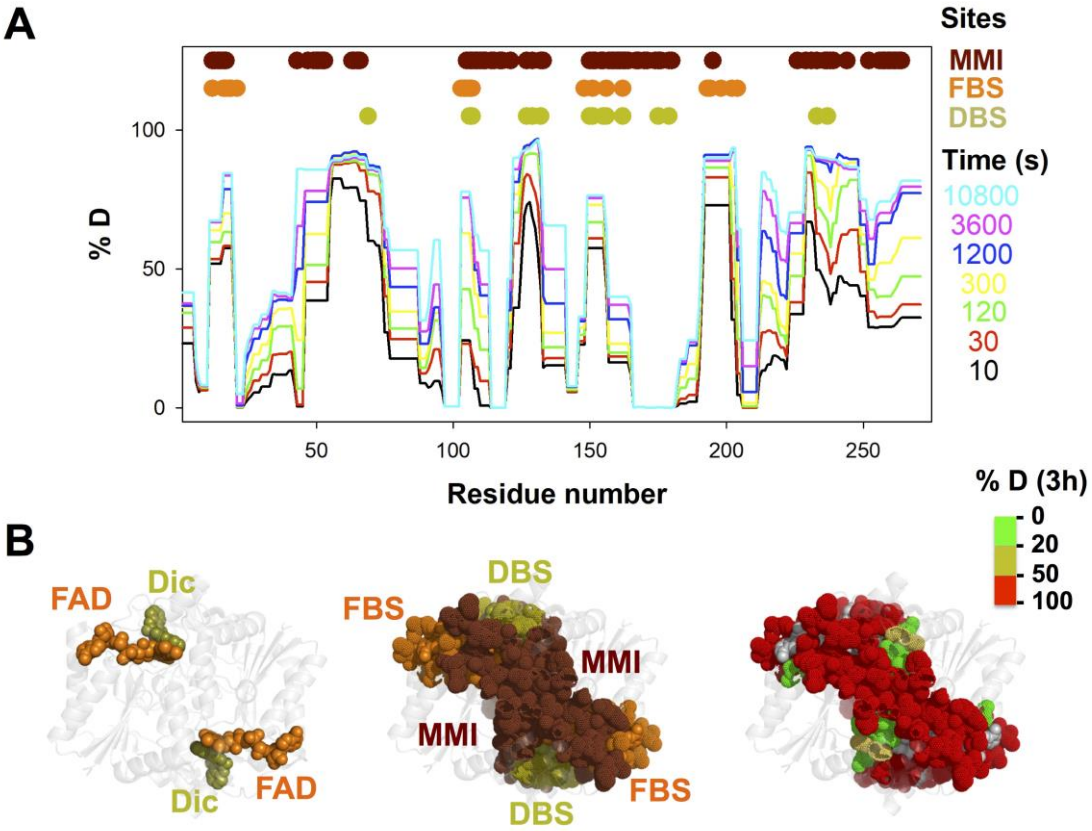

Figure 1. Overall HDX kinetics of NQO1$_{apo}$. (**A**) Time-dependent HDX kinetics for segments of NQO1$_{apo}$. Residues belonging to the monomer:monomer interface (MMI), FAD binding site (FBS) and dicoumarol binding site (DBS) are indicated as coloured circles. These sites were retrieved from the analysis of the NQO1 structure (PDB 2F1O; [15]) using the PISA server (https://www.ebi.ac.uk/pdbe/pisa/); (**B**) Structural representation of HDX after 3h [%D (3h)] in NQO1$_{apo}$. For visual aid, the left panel shows the location of bound FAD and dicoumarol, the middle panel shows those residues belonging to the MMI, FBS and DBS, and the right panel displays the %D after 3 h for residues belonging to these functional sites.

Within non-exchanging segments, we found that these contained mostly residues buried in the crystallographic structure of NQO1 (in a ternary complex with FAD and dicoumarol bound, PDB 2F1O; NQO1$_{dic}$) (Figure 2A). Thus, these sequences likely represent regions that are critical for the acquisition and maintenance of a minimally stable dimeric fold NQO1$_{apo}$ (note that NQO1$_{apo}$ is dimeric in solution but more expanded and flexible, and with lower conformational stability than NQO1$_{holo}$ [9, 14]). This minimal core involves helices α1, α3 and α4 and sheets β1 and β3-β5 (Figure 2A and S7). This core may also contribute to the acquisition of a minimally folded monomeric state that becomes stabilized in the dimeric state by the interactions between helices α3 and α4 across the monomers (i.e. the MMI)(Figure 2B and S7).

Preprints (www.preprints.org) | NOT PEER-REVIEWED | Posted: 24 October 2019 doi:10.20944/preprints201910.0281.v1

Peer-reviewed version available at Biomolecules 2019, 9, 728; doi:10.3390/biom9110728

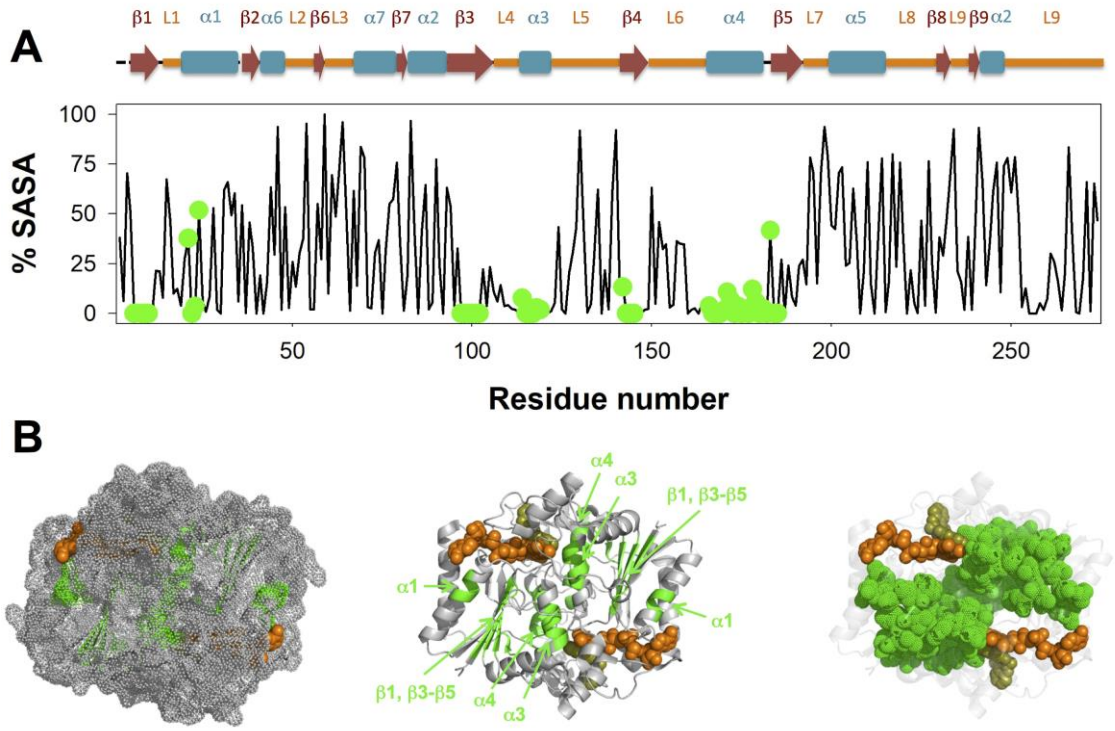

Figure 2. ***Non-exchanging*** **segments define a minimal stable core in NQO1apo.** (**A**) Plot of the % SASA (solvent accesible surface area) for individual residues (considering backbone and side-chain) calculated from the structure of NQO1dic (PDB 2F1O [15]) using GETAREA (http://curie.utmb.edu/getarea.html; This algorithm do not consider the ligands in the calculation). Secondary structure elements are depicted according to [11]; Residues belonging to non-exchanging segments are displayed as green circles; (**B**) Structural representation of non-exchanging segments (using PDB 2F1O; [15]). The left panel shows a surface representation highlighting the burial of the minimal and stable core. The middle panel shows segments belonging to this core plotted onto secondary structure elements. The right panel shows that this core may contribute to the stable folding of the individual monomers as well as their assembly into the dimer, with only few stable contacts with the FAD (in orange ball representation) and the dicoumarol (in yellow ball representation).

Importantly, the FBS and DBS in NQO1apo are overall exchanging (Figure 1B, 2B and S7B), with the main exceptions being some marginal contacts in helices α1 and α3 (FBS) and α4 (DBS)(Figure 2B ans S7B). Thus, our HDX analyses support that the conformational ensemble of NQO1apo is essentially populated by states non-competent for FAD or dicoumarol binding due to the high structural dynamics of their binding sites [9, 14, 34].

3.2. Complex HDX kinetics

To provide deeper insight into the structural dynamics of NQO1apo, we carefully analyzed the HDX kinetics for all protein segments (Figure S5). It should be noted that these HDX kinetics were very consistent with those obtained directly from peptides experimentally characterized (Figure S6 and S10). For the majority of the cases, HDX kinetics was described very well by a simple function with two kinetic phases (see Figure S5-S6 for fittings, and Table S1-S2 for the best-fit values): a burst-phase corresponding to HDX mostly occurring within the experimental dead time (i.e. very few seconds), and thus characterized by a single parameter: its amplitude A_{burst}; and a slow phase that occurred typically in a scale of several seconds to minutes, characterized by two parameters: its amplitude A_{slow} and an apparent first-order rate constant (k_{slow}), following this equation:

$$\%\, D(t) = A_{burst} + A_{slow} \cdot (1 - exp^{-k_{slow} \cdot t})$$

We chose to use this phenomenological description of HDX kinetics mainly for two reasons. First, it provided a simple scenario from which, using three characteristic parameters (A_{burst}, A_{slow} and k_{slow}) we could compare the HDX kinetics of different segments of $NQO1_{apo}$ (see Figure 3; note that this approach worked also very well with the HDX kinetics of $NQO1_{holo}$ and $NQO1_{dic}$; see Figure S5-S6 and Table S1-S2). Second, although the HDX kinetics analyzed using more complex functions (e.g. the two kinetic phases containing each a characteristic rate constant) may provide in some cases better fits, this would put the analyses at two intertwined risks: increasing the fitting parameters would make comparisons between behaviors more difficult, and importantly, in many cases these fittings show evident signs of overparametrization.

Kinetic analyses of HDX for protein segments considered as exchanging (> 20%D after 3 h) revealed certain interesting behaviours. First, for many protein segments (of different lengths), we observed a significant contribution to the HDX kinetics from both the burst and slow phases (Figure 3 and S8, and Table S1-S2). As indicated above, the HDX kinetics of NQO1 in all three ligation states is vastly consistent with EX2 kinetics, and thus, the observed kinetics depends to some extent on the equilibrium constant between non-exchanging and exchanging states [40]. Therefore, the presence of two clearly differentiated kinetic phases suggests the existence of complexity (i.e. heterogeneity) in the conformational ensemble of $NQO1_{apo}$, and plausibly, the significant population of at least two conformational substates with different HDX behavior which may or may not significantly reequilibrate upon the intrinsic HDX step. Interestingly, although ligand binding affects these two kinetic phases ($NQO1_{holo}$ and $NQO1_{dic}$, see Figure S5-S6 and Table S1-S2), both these phases still contribute to the HDX kinetics in these ligation states, suggesting that certain degree of conformational heterogeneity remains upon ligand binding. Second, although in the EX2 scenario the overall kinetics depends on the intrinsic HDX rate constant, and therefore, on the individual backbone amides and their vicinity [40], some sort of correlated behavior at larger scales than small protein segments (e.g. secondary structure elements) is observed (Figure 3B and S8). Consistent with the above-mentioned proposal of a stable core of $NQO1_{apo}$ with highly dynamic FBS and DBS (simply made by analysis of % D after 3 h, Figure 2), these kinetic analyses suggest that secondary structure elements outside the stable core typically exchanged quite fast (i.e. with large burst phases and with k_{slow} often in the range of 10^{-1} to 10^{-2} s^{-1}; Figure 3B and S8).

Preprints (www.preprints.org) | NOT PEER-REVIEWED | Posted: 24 October 2019 doi:10.20944/preprints201910.0281.v1

Peer-reviewed version available at Biomolecules 2019, 9, 728; doi:10.3390/biom9110728

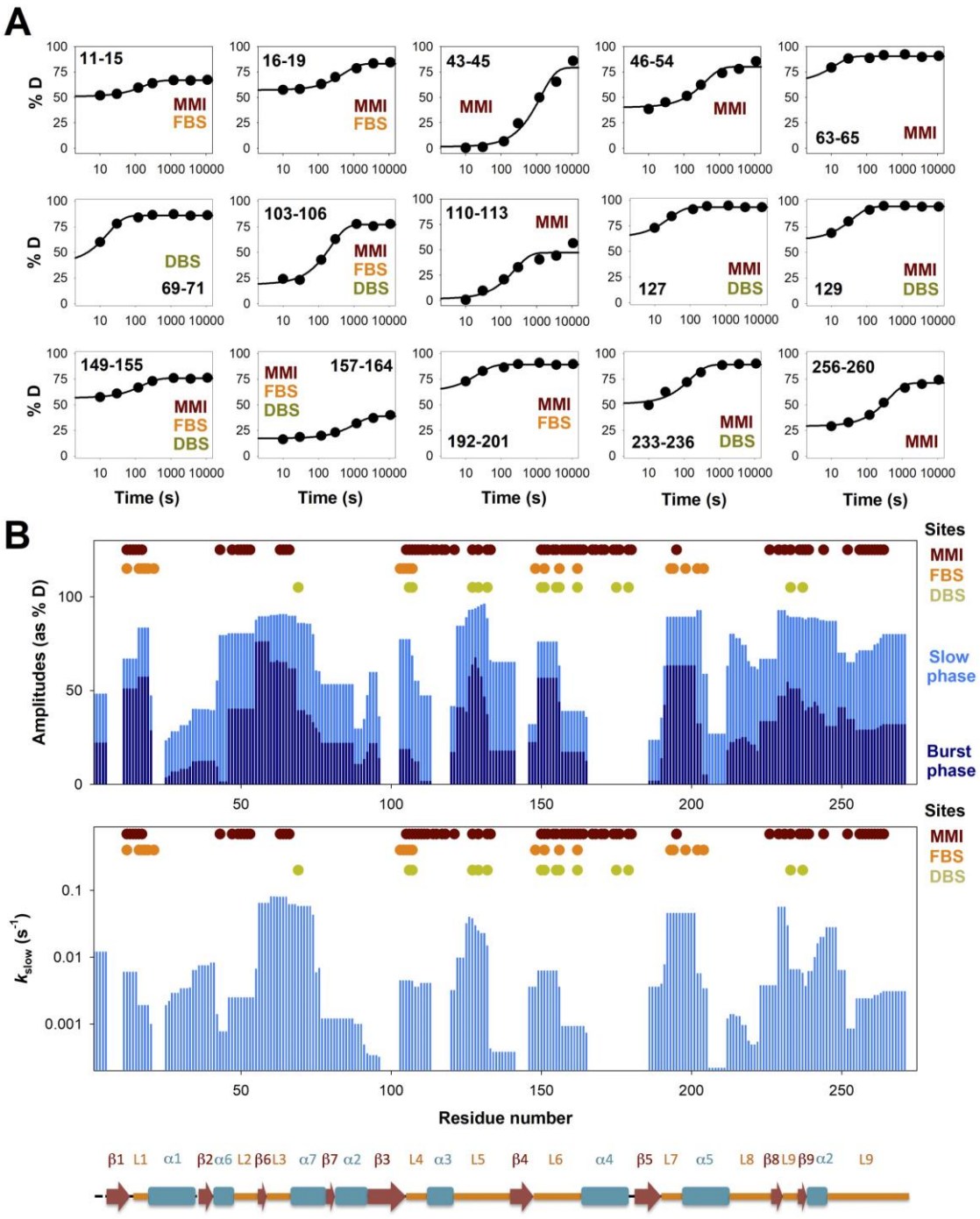

Figure 3. Segment-specific HDX kinetics of NQO1$_{apo}$. (**A**) Fittings of HDX kinetics for selected segments typically showing at least 50 % D incorporation after 3h and considered part of the functional sites (MMI, FBS and DBS). (**B**) Plots of the amplitudes for the burst- and slow-phase in HDX for segments (upper panel) and rate constant for the slow phase (lower panel) for segments with at least 20% D after 3 h. The elements of secondary structure along the protein sequence are also indicated.

Preprints (www.preprints.org) | NOT PEER-REVIEWED | Posted: 24 October 2019 doi:10.20944/preprints201910.0281.v1

Peer-reviewed version available at Biomolecules 2019, 9, 728; doi:10.3390/biom9110728

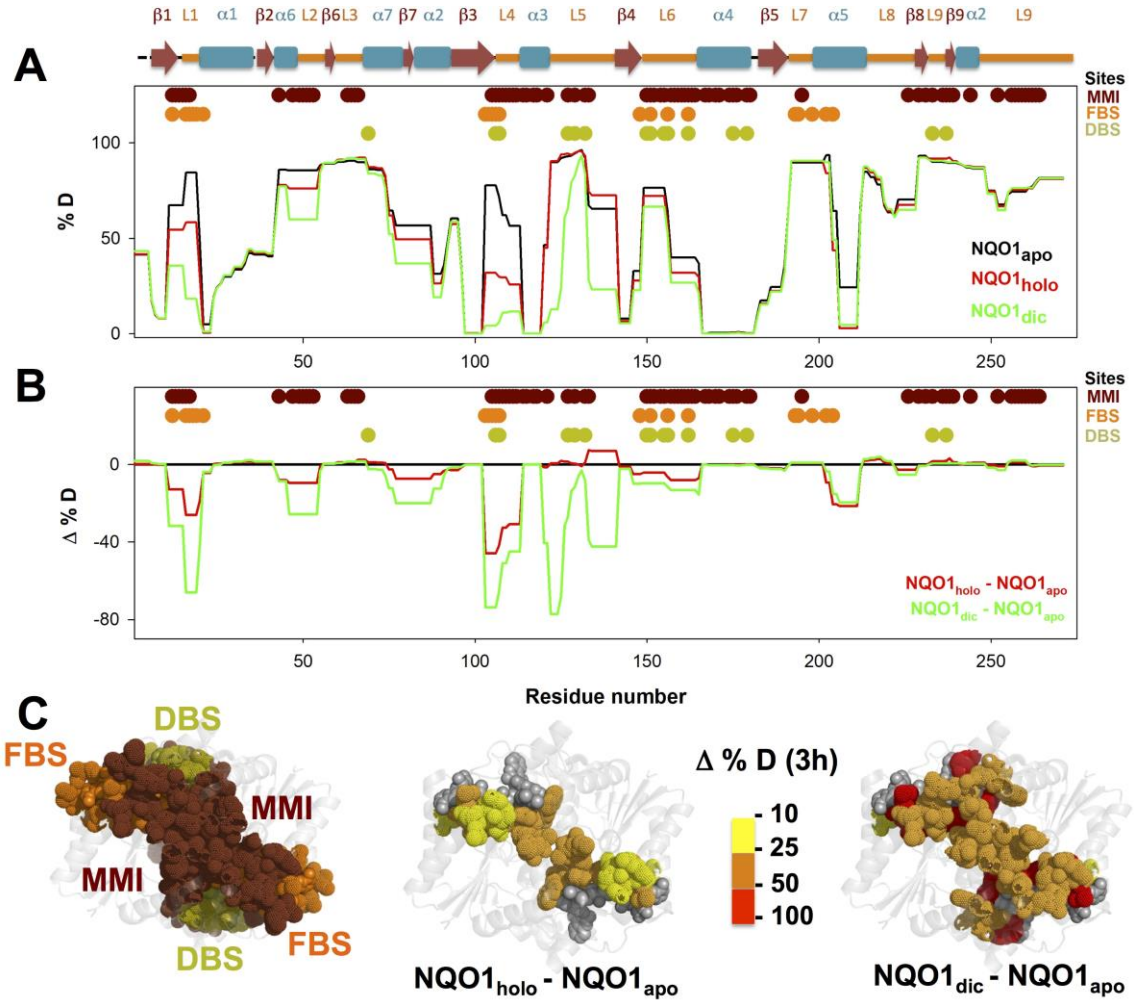

Figure 4. Overall HDX kinetics for segments of NQO1 upon binding FAD and dicoumarol. (**A and B**) HDX for segments of $NQO1_{apo}$, $NQO1_{holo}$ and $NQO1_{dic}$. Panel A shows % D after 3 h and Panel B the difference in this parameter between $NQO1_{holo}$ or $NQO1_{dic}$ and $NQO1_{apo}$. Residues belonging to the MMI, FBS and DBS were indicated (retrieved as described in Figure 2). (**C**) % D after 3h in NQO1 upon FAD and dicoumarol binding plotted onto the NQO1 structure (PDB 2F1O). For comparison, the left panel shows the location of MMI, FBS and DBS, the middle and right panels show those residues belonging to the these sites that displayed at least a decrease of 10% D after 3 h in $NQO1_{holo}$ (middle panel) or $NQO1_{dic}$ (right panel) vs. $NQO1_{apo}$.

3.3. FAD and dicoumarol binding cause large-scale changes in protein structural dynamics

FAD binding to $NQO1_{apo}$ is known to cause significant overall changes in protein structure and dynamics: it increases the content in ordered secondary structure, reduces the protein hydrodynamic volume, and substantially enhances protein stability and resistance towards proteolytic attack [9, 14, 22, 34, 35]. In addition, structural and biophysical analyses have shown that NQO1 must contain bound FAD in order to bind dicoumarol with high affinity [9, 14]. We first compared the % D incorporated to $NQO1_{holo}$ and $NQO1_{apo}$ after 3h of reaction (Figure 4A-B), observing some interesting changes upon FAD binding. Particularly large differences were observed in loop L1 (involved in the MMI and the FBS), loop L4 (involved in the MMI, the FBS and the DBS) and helix α5 (involved in the FBS). The stabilization observed for the MMI thus explain the increased thermostability of the NQO1 dimer upon FAD binding. The much lower structural dynamics of the FBS upon FAD binding is also consistent with a induced-fit mechanism, in which binding competent states (with high structural stability) are marginally populated in the absence of FAD, according to a recent proposal based on binding structure-thermodynamic relationships [34]. Interestingly, these results also imply that FAD is not only required for dicoumarol binding as a part of the DBS, but also

Preprints (www.preprints.org) | NOT PEER-REVIEWED | Posted: 24 October 2019 doi:10.20944/preprints201910.0281.v1

Peer-reviewed version available at Biomolecules 2019, 9, 728; doi:10.3390/biom9110728

that FAD binding modifies the dynamics of protein structural elements involved in the binding of the inhibitor (Figure 4C). It is worth noting that FAD binding also slows down signficantly (3- to 5-fold) HDX of other regions such as sheet β6, helix α7 and loop L3 (Figure 5 and S5, and Table S1), some of them not directly involved in the MMI, FBS or DBS.

Dicoumarol binding to $NQO1_{holo}$ is also known to increase the protein ordered secondary structure, thermal stability and resistance of N-terminal domain towards proteolysis [9, 14]. According to this evidence, we observed that dicoumarol binding to $NQO1_{holo}$ decreased the % D after 3 h even to a larger extent than FAD binding, and these effects seemed to propagate to more distant regions in the protein structure, extensively affecting regions involved in the MMI, the FBS and DBS (Figure 4). The regions affected by dicoumarol binding actually affected the very same set of structural regions affected by FAD binding with the exception of helix α5 (Figure 4). In contrast to FAD, dicoumarol binding also caused a dramatic reduction of % D in sheet β4 and loop L5, that contain residues belonging to the MMI and the DBS (Figure 4). In addition, dicoumarol binding slowed down the HDX kinetics of helix α7 and loops L4 and L5 (Figure 5 and S5-S6, and Table S1-S2) by several orders of magnitude.

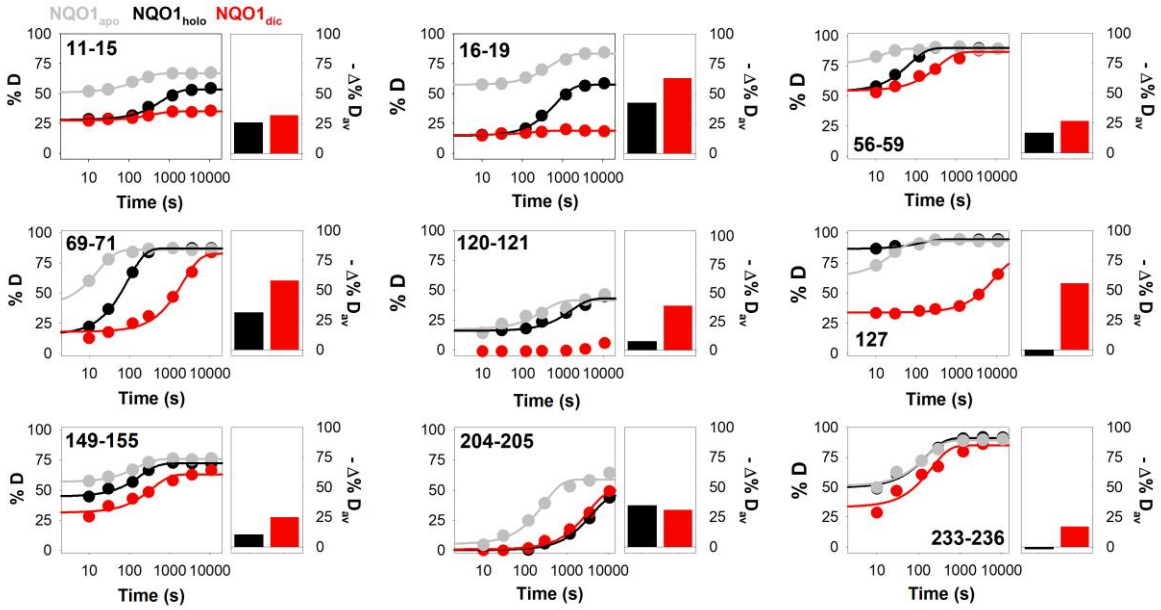

Figure 5. Changes in segment-specific HDX kinetics of NQO1 upon FAD and dicoumarol binding. Right panels show fittings of HDX kinetics for selected individual segments using a single exponential function with a burst-phase for $NQO1_{apo}$ (grey), $NQO1_{holo}$ (black) and $NQO1_{dic}$ (red). These data were used to calculate $\Delta\%D_{av}$, as average of the time points with maximal differences between a given NQO1 form ($NQO1_{holo}$, black; $NQO1_{dic}$, red) and $NQO1_{apo}$, as a single metric to quantify changes in HDX kinetics (left panels).

Clearly, the HDX kinetics of NQO1 in all three ligation states ($NQO1_{apo}$, $NQO1_{holo}$ and $NQO1_{dic}$) were overall complex (Figure 5 and S5-S6). Therefore, it was not straightforward to provide a single metric from the global kinetic analysis reported so far in this work, even when a simple kinetic model was used. To quantify the effects of ligand binding (and potentially of mutations) on the structural dynamics of NQO1, we sought for a single metric that would respond, at least semi-quantitatively, to the different types of change observed upon ligand binding (Figure 4 and 5). We must note that these changes include a variety of effects on the amplitudes of the two kinetic phases (sometimes increasing, decreasing, not changing or even shifting between the amplitudes of the burst and the slow phases upon ligand binding) and also on the rate constant of the slow phase (in some cases this phase was too fast or slow to be measured adequately)(see Table S1 and S2). Notably, all these effects on the HDX kinetics can be simplified to a common effect: at least a few of

Preprints (www.preprints.org) | NOT PEER-REVIEWED | Posted: 24 October 2019 doi:10.20944/preprints201910.0281.v1

Peer-reviewed version available at Biomolecules 2019, 9, 728; doi:10.3390/biom9110728

the data in the time-dependent measurements differ from two samples when these samples are paired for a given time point (see Figure 5 for representative examples). Thus, we decided to simply calculate the difference between the two paired proteins species for a given time and protein segment, and for each segment, to average the three time points with a maximal difference in these time series. Indeed, this simple metric (called $\Delta\%D_{av}$) was able to detect and rank the effects of ligand binding on NQO1 HDX due to changes in amplitudes and kinetic rate constants (Figure 5).

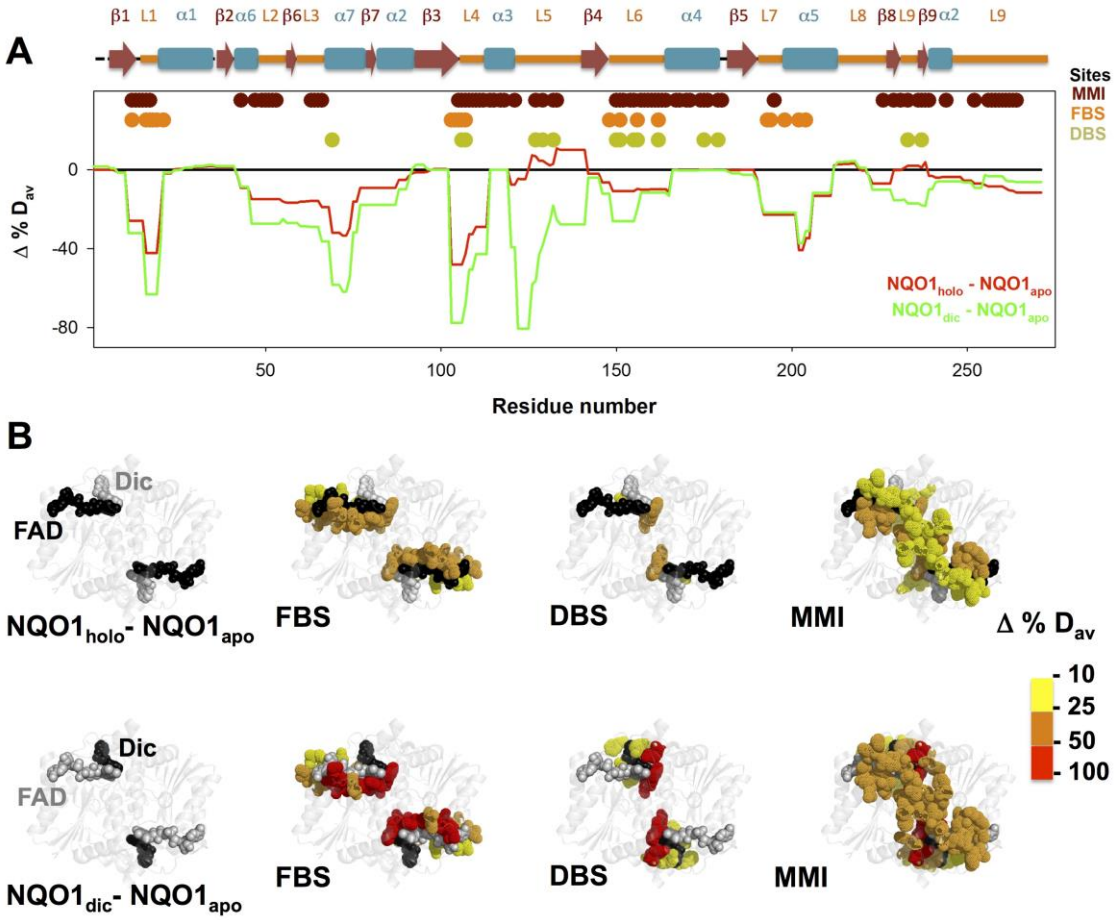

Figure 6. Changes in HDX kinetics of NQO1 upon binding FAD and dicoumarol as changes in %D_{av} ($\Delta\%D_{av}$). A) $\Delta\%D_{av}$ for NQO1 segments upon binding FAD ($NQO1_{holo}$) and dicoumarol ($NQO1_{dic}$) using of $NQO1_{apo}$ as a reference. Residues belonging to the MMI, FBS and DBS are indicated (retrieved as in Figure 2). B) Representation of ($\Delta\%D_{av}$) onto the structure of NQO1 (using PDB code 2F1O). The upper row shows results for $\Delta\%D_{av}$ for $NQO1_{holo}$ and the lower row represents $NQO1_{dic}$. Different panels in each row show results for residues involved in the FBS, DBS or MMI.

We compared again the behavior of $NQO1_{holo}$ vs. $NQO1_{apo}$ using $\Delta\%D_{av}$ (Figure 6A and S9A). The results showed that FAD binding substantially reduced the backbone dynamics of residues 11-20 (loop L1 and helix α1), 46-76 (loops L2 and L3, helix α7 and sheet β6), 103-113 (sheet β6 and loop L4), 149-165 (loop L6) and 191-211 (loop L7 and helix α5)(Figure 6A). These regions include most of the residues involved in the MMI and FBS, and also some belonging to the DBS (Figure 6A-B). When we evaluated the effect of dicoumarol binding, we observed further structural stabilization of all these regions (with the exception of residues 191-211) and a specific stabilization of two additional regions mostly involved in the MMI and DBS,: i) a dramatic stabilization of the segment 120-141 (loop 5); ii) a moderate effect in the segment 223-240 (loops L8 and and L9 and sheet β8 and β9).

3.4. Insights into cooperative effects upon FAD and dicoumarol binding from analysis of structural dynamics

In addition to the overall conformational and functional consequences of FAD and dicoumarol binding to NQO1, some experimental techniques have revealed some complexity in the functional chemistry of this enzyme [22, 23, 41]. This behavior is not unexpected since binding of FAD to $NQO1_{apo}$ and dicoumarol to $NQO1_{holo}$ is described by a general formalism for binding of a ligand (L) to a macromolecule (P, NQO1 dimer) with two binding sites (Scheme 2) [42]:

Scheme 2. General formalism for a macromolecule P (NQO1 dimer) with two ligand (L) binding sites.

in which K_1 and K_2 describe the step-wise equilibrium constants as follows:

$$K_1 = \frac{[PL]}{[P] \cdot [L]}$$

$$K_2 = \frac{[PL_2]}{[PL] \cdot [L]}$$

For a P with two equivalent and non-interacting binding sites, these two step-wise equilibrium binding constants are related through a simple relationship: $4 \cdot K_1 = K_2$. Significant deviations from this relationship imply the existence of non-equivalent or interacting sites: $4\ K_1 > K_2$ implies either negative cooperativity or non-equivalent binding sites, while $4\ K_1 < K_2$ unequivocally identifies positive cooperativity. It must be noted that, in this scenario, the largest differences between cooperative and non-cooperative binding are found for the dependence of the population of the half-ligated species PL (e.g. NQO1 dimer with one FAD bound) on [L] [22, 23, 42].

The NQO1 dimer contains two binding sites for either FAD or dicoumarol. Interestingly, calorimetric titrations of $NQO1_{apo}$ with FAD and $NQO1_{holo}$ with dicoumarol, as well as inhibition studies in the case of dicoumarol, have identified the existence of negative cooperativity in the binding of both ligands [22, 23, 41]. A detailed structural characterization of the communication between ligand binding sites underlying these cooperative effects are challenging for several reasons. First, in the ligand binding equilibrium, the unligated (P), half-ligated (PL) and fully-ligated (PL_2) species contribute structurally and energetically to the observed cooperative binding. However, to date, no structural information of the P or PL states for FAD binding are available (i.e. no high-resolution structure of $NQO1_{apo}$ or the intermediate species with a single FAD molecule bound per dimer), while for dicoumarol binding no structural information for PL ($NQO1_{holo}$ with a single dicoumarol molecule bound per dimer) is available. Although our current HDXMS study does not report on half-ligated species, we were capable of identifying a network of interacting residues in $NQO1_{apo}$ that connect structurally and energetically the FBS and the DBS between monomers through the MMI interface. Therefore, our results suggest the existence of a highly dynamic structural network connecting these binding sites between the monomers in NQO1, and these results may also provide a blueprint for future experimental and computational mutagenesis studies aimed at perturbing and analyzing the role of this network in ligand binding energetics and cooperativity. In support of this hypothesis, recent work has shown that the Gly151Ser mutation (Gly150 according to the crystal structure) essentially prevents the communication of ligand binding effects between the two DBS across the NQO1 dimer [41]. Gly151 is located in the begining of loop L6, and it undergoes a noticeable decrease in structural dynamics upon dicoumarol binding (Figure 6), which might constitute part of the allosteric signal generated by dicoumarol binding to one site (to form the half-ligated state PL) that communicates to the other subunit contributing to the negative cooperativity for dicoumarol binding. More globally, our analyses from HDXMS support the idea that dicoumarol binding triggers changes in NQO1 dynamics for certain (but not all)

Peer-reviewed version available at Biomolecules 2019, 9, 728; doi:10.3390/biom9110728

regions predicted by studies using a Gaussian network approach on structural models for the P and PL states [41]. In agreement with this recent study, we observed that dicoumarol binding affected the dynamics of loops L3 and L5, sheets β6 and β7, and helices α2, α5 and α7, which showed the largest changes in dynamics when the slowest frequency modes were analyzed upon formation of the PL state by a Gaussian network model (Figure 6 vs. [41]).

4. Conclusions

The multifunctional nature of NQO1 is likely controlled, to a large extent, by changes in protein structural dynamics triggered by the binding of small molecules (FAD, NAD(P)H, substrates, inhibitors) as well as by interaction with other biomacromolecules (proteins and nucleic acids). These structural and energetic aspects are critical to improve our understanding of these interactions under physiological and pathological conditions. In this work, we showed that the use of HDXMS can be instrumental to provide unprecedented detail of the effects of ligand binding on the functional chemistry of NQO1 linked to changes in protein structural dynamics. This approach may provide novel insights into the regulation of NQO1 activity and stability *in vivo*, as well as the mechanisms by which these properties are regulated and/or dysregulated by disease-associated single amino acid exchanges and post-translational modifications.

NQO1 is one of the human flavoproteins for which intracellular protein levels are more strongly coupled to intracellular availability of the flavin cofactor [25]. Our current understanding of this phenomenon proposes that this sensitivity of protein stability is due to efficient recognition and degradation of human apo-flavoproteins by the ubiquitin-dependent proteasomal pathway [14, 25, 30]. The lack of high resolution information on the structure and dynamics of human apo-flavoproteins, due to the instability of these apo-proteins, has prevented us from a deep understanding of these recognition mechanisms. The detailed analysis reported herein for $NQO1_{apo}$ support that HDXMS can be also used to improve our understanding of this phenomenon as well as the mechanisms by which disease-associated mutations and post-translational modifications may alter protein structural dynamics leading to alternative recognition mechanisms by the proteasomal degradation pathway [14, 30, 34, 36].

In this work we identified a minimally stable core that allows $NQO1_{apo}$ to exist as a dimer, although this dimer constitutes a highly dynamic conformational ensemble and with marginal conformational stability. This core may serve as a wiring network that allows communication of ligand binding and mutational effects between domains and between subunits through this minimally stable MMI (see [9, 22, 23, 32, 33] and cooperative effects upon FAD and dicoumarol binding [22, 23, 41].

Our study also allows us to discuss the deleterious effects of the common cancer-associated polymorphism Pro187Ser. Pro187 belongs to sheet β5, as a part of the stable core of the monomer in $NQO1_{apo}$ state (Figure 2). Thus, the strong structural perturbation presumably caused by the Pro187Ser substitution could readily cause long-range effects on the structural dynamics of $NQO1_{apo}$ by disrupting this stable core, and these effects could propagate within the monomer and between subunits in the dimer. This interpretation agrees with previous experimental, computational and structural perturbation analyses carried out on the Pro187Ser variant [5, 14, 22, 30, 32, 33, 34, 36]. Consequently, even in the $NQO1_{apo}$, the cancer-associated polymorphism Pro187Ser would destabilize the NQO1 monomer and this effect could easily propagate to the MMI, the FBS and the DBS, thus contributing to explain the low conformational stability of P187S *in vitro*, its low affinity for FAD and dicoumarol and its accelerated degradation by the proteasome [9, 10, 14, 22, 23, 24, 25, 34].

Our analyses also support that HDXMS can provide unprecedented structural insight into the catalytic cycle of NQO1. First, our results indicate that FAD binding shifts the conformational

ensemble of NQO1 towards more stable and competent states for either NAD(P)H or dicoumarol binding (i.e. at the DBS). This effect is further strengthened upon binding of the inhibitor, suggesting that the structural dynamics of the DBS (and plausibly of the NAD(P)H binding site; [15]) acts by limiting the available ligand binding poses of NAD(P)H. This would optimize hydride transfer from the adenine dinucleotide coenzyme to the FAD, thus contributing to high rate constants experimentally measured for the reductive half-reaction catalyzed by NQO1 [10].

Supplementary Materials: The following are available online. In the Supplementary information file, Figure S1-S10 and Tables S1 and S2 can be found.

Author Contributions: conceptualization, A.L.P; methodology, P.V., P.M and A.L.P.; software, P.V. and P.M; validation, P.V., P.M. and A.L.P; formal analysis, P.V., P.M. and A.L.P; investigation, P.V., E.S., P.M. and A.L.P; resources, E.S., P.M. and A.L.P; data curation, P.V., D.J.T., P.M. and A.L.P; writing-original draft preparation, P.V., P.M. and A.L.P; writing-review and editing, P.V., E.S., D.J.T., P.M. and A.L.P; visualization, P.M. and A.L.P.; supervision, P.M. and A.L.P.; project administration, P.M. and A.L.P; funding acquisition, E.S., P.M. and A.L.P.

Funding: This research was funded by the ERDF/Spanish Ministry of Science, Innovation and Universities - State Research Agency (Grant RTI2018-096246-B-I00, to A.L.P.), the Spanish Ministry of Economy and Competitiveness (Grant SAF2015-69796 to E.S.) and Junta de Andalucía (Grant P11-CTS-07187, to ALP).

Acknowledgments: We acknowledged assistance from Dr. Noel Mesa-Torres in protein expression and purification. Access to a EU_FT-ICR_MS network installation was funded by the EU Horizon 2020 grant 731077. Additional support from Aula FUNCANIS-UGR, EU and MEYS CZ funds CZ.1.05/1.1.00/02.0109, LQ1604 and LM2015043 is gratefully acknowledged.

Conflicts of Interest: The authors declare no conflict of interest.

References

1. Beaver, S.K.; Mesa-Torres, N.; Pey, A.L.; Timson, D.J. NQO1: A target for the treatment of cancer and neurological diseases, and a model to understand loss of function disease mechanisms. *Biochim Biophys Acta Proteins Proteom* 2019, *1867*, 663-676.

2. Ross, D.; Siegel, D. Functions of NQO1 in Cellular Protection and CoQ10 Metabolism and its Potential Role as a Redox Sensitive Molecular Switch. *Front Physiol* 2017, *8*, 595.

3. Ross, D.; Siegel, D. NQO1 in protection against oxidative stress. *Current Opinion in Toxicology* 2018, *7*, 67-72.

4. Pey, A.L.; Megarity, C.F.; Medina-Carmona, E.; Timson, D.J. Natural Small Molecules as Stabilizers and Activators of Cancer-Associated NQO1 Polymorphisms. *Curr Drug Targets* 2016, *17*, 1506-1514.

5. Pey, A.L.; Megarity, C.F.; Timson, D.J. NAD(P)H quinone oxidoreductase (NQO1): an enzyme which needs just enough mobility, in just the right places. *Biosci Rep* 2019, *39*.

6. Dinkova-Kostova, A.T.; Talalay, P. NAD(P)H:quinone acceptor oxidoreductase 1 (NQO1), a multifunctional antioxidant enzyme and exceptionally versatile cytoprotector. *Arch Biochem Biophys* 2010, *501*, 116-123.

7. Siegel, D.; Gustafson, D.L.; Dehn, D.L.; Han, J.Y.; Boonchoong, P.; Berliner, L.J.; Ross, D. NAD(P)H:quinone oxidoreductase 1: role as a superoxide scavenger. *Mol Pharmacol* 2004, *65*, 1238-1247.

8. Siegel, D.; Dehn, D.D.; Bokatzian, S.S.; Quinn, K.; Backos, D.S.; Di Francesco, A.; Bernier, M.; Reisdorph, N.; de Cabo, R.; Ross, D. Redox modulation of NQO1. *PLoS One* 2018, *13*, e0190717.

9. Medina-Carmona, E.; Neira, J.L.; Salido, E.; Fuchs, J.E.; Palomino-Morales, R.; Timson, D.J.; Pey, A.L. Site-to-site interdomain communication may mediate different loss-of-function mechanisms in a cancer-associated NQO1 polymorphism. *Scientific Reports* 2017, *7*, 44352.

10. Lienhart, W.D.; Gudipati, V.; Uhl, M.K.; Binter, A.; Pulido, S.A.; Saf, R.; Zangger, K.; Gruber, K.; Macheroux, P. Collapse of the native structure caused by a single amino acid exchange in human NAD(P)H:quinone oxidoreductase(1.). *FEBS J* 2014, *281*, 4691-4704.

11. Faig, M.; Bianchet, M.A.; Talalay, P.; Chen, S.; Winski, S.; Ross, D.; Amzel, L.M. Structures of recombinant human and mouse NAD(P)H:quinone oxidoreductases: species comparison and structural changes with substrate binding and release. *Proc Natl Acad Sci U S A* 2000, *97*, 3177-3182.

12. Li, R.; Bianchet, M.A.; Talalay, P.; Amzel, L.M. The three-dimensional structure of NAD(P)H:quinone reductase, a flavoprotein involved in cancer chemoprotection and chemotherapy: mechanism of the two-electron reduction. *Proc Natl Acad Sci U S A* 1995, *92*, 8846-8850.

13. Chen, S.; Deng, P.S.; Bailey, J.M.; Swiderek, K.M. A two-domain structure for the two subunits of NAD(P)H:quinone acceptor oxidoreductase. *Protein Sci* 1994, *3*, 51-57.

14. Medina-Carmona, E.; Palomino-Morales, R.J.; Fuchs, J.E.; Padín-Gonzalez, E.; Mesa-Torres, N.; Salido, E.; Timson, D.J.; Pey, A.L. Conformational dynamics is key to understanding loss-of-function of NQO1 cancer-associated polymorphisms and its correction by pharmacological ligands. *Scientific Reports* 2016, *6*, 20331.

15. Asher, G.; Dym, O.; Tsvetkov, P.; Adler, J.; Shaul, Y. The crystal structure of NAD(P)H quinone oxidoreductase 1 in complex with its potent inhibitor dicoumarol. *Biochemistry* 2006, *45*, 6372-6378.

16. Moscovitz, O.; Tsvetkov, P.; Hazan, N.; Michaelevski, I.; Keisar, H.; Ben-Nissan, G.; Shaul, Y.; Sharon, M. A mutually inhibitory feedback loop between the 20S proteasome and its regulator, NQO1. *Mol Cell* 2012, *47*, 76-86.

17. Asher, G.; Tsvetkov, P.; Kahana, C.; Shaul, Y. A mechanism of ubiquitin-independent proteasomal degradation of the tumor suppressors p53 and p73. *Genes Dev* 2005, *19*, 316-321.

18. Oh, E.T.; Kim, J.W.; Kim, J.M.; Kim, S.J.; Lee, J.S.; Hong, S.S.; Goodwin, J.; Ruthenborg, R.J.; Jung, M.G.; Lee, H.J.; Lee, C.H.; Park, E.S.; Kim, C.; Park, H.J. NQO1 inhibits proteasome-mediated degradation of HIF-1alpha. *Nat Commun* 2016, *7*, 13593.

19. Lata, S.; Ali, A.; Sood, V.; Raja, R.; Banerjea, A.C. HIV-1 Rev downregulates Tat expression and viral replication via modulation of NAD(P)H:quinine oxidoreductase 1 (NQO1). *Nat Commun* 2015, *6*, 7244.

20. Di Francesco, A.; Di Germanio, C.; Panda, A.C.; Huynh, P.; Peaden, R.; Navas-Enamorado, I.; Bastian, P.; Lehrmann, E.; Diaz-Ruiz, A.; Ross, D.; Siegel, D.; Martindale, J.L.; Bernier, M.; Gorospe, M.; Abdelmohsen, K.; de Cabo, R. Novel RNA-binding activity of NQO1 promotes SERPINA1 mRNA translation. *Free Radic Biol Med* 2016, *99*, 225-233.

21. Betancor-Fernandez, I.; Timson, D.J.; Salido, E.; Pey, A.L. Natural (and Unnatural) Small Molecules as Pharmacological Chaperones and Inhibitors in Cancer. *Handb Exp Pharmacol* 2018, *45*, 345-383.

22. Pey, A.L.; Megarity, C.F.; Timson, D.J. FAD binding overcomes defects in activity and stability displayed by cancer-associated variants of human NQO1. *Biochim Biophys Acta* 2014, *1842*, 2163-2173.

23. Claveria-Gimeno, R.; Velazquez-Campoy, A.; Pey, A.L. Thermodynamics of cooperative binding of FAD to human NQO1: Implications to understanding cofactor-dependent function and stability of the flavoproteome. *Arch Biochem Biophys* 2017, *636*, 17-27.

24. Siegel, D.; Anwar, A.; Winski, S.L.; Kepa, J.K.; Zolman, K.L.; Ross, D. Rapid polyubiquitination and proteasomal degradation of a mutant form of NAD(P)H:quinone oxidoreductase 1. *Mol Pharmacol* 2001, *59*, 263-268.

25. Martinez-Limon, A.; Alriquet, M.; Lang, W.H.; Calloni, G.; Wittig, I.; Vabulas, R.M. Recognition of enzymes lacking bound cofactor by protein quality control. *Proc Natl Acad Sci U S A* 2016, *113*, 12156-12161.

26. Luo, S.; Su Kang, S.; Wang, Z.H.; Liu, X.; Day, J.X.; Wu, Z.; Peng, J.; Xiang, D.; Springer, W.; Ye, K. Akt Phosphorylates NQO1 and Triggers its Degradation, Abolishing its Antioxidative Activities in Parkinson's Disease. *J Neurosci* 2019.

27. Nolan, K.A.; Scott, K.A.; Barnes, J.; Doncaster, J.; Whitehead, R.C.; Stratford, I.J. Pharmacological inhibitors of NAD(P)H quinone oxidoreductase, NQO1: structure/activity relationships and functional activity in tumour cells. *Biochem Pharmacol* 2010, *80*, 977-981.

28. Nolan, K.A.; Zhao, H.; Faulder, P.F.; Frenkel, A.D.; Timson, D.J.; Siegel, D.; Ross, D.; Burke, T.R., Jr.; Stratford, I.J.; Bryce, R.A. Coumarin-based inhibitors of human NAD(P)H:quinone oxidoreductase-1. Identification, structure-activity, off-target effects and in vitro human pancreatic cancer toxicity. *J Med Chem* 2007, *50*, 6316-6325.

29. Scott, K.A.; Barnes, J.; Whitehead, R.C.; Stratford, I.J.; Nolan, K.A. Inhibitors of NQO1: identification of compounds more potent than dicoumarol without associated off-target effects. *Biochem Pharmacol* 2011, *81*, 355-363.

30. Medina-Carmona, E.; Rizzuti, B.; Martin-Escolano, R.; Pacheco-Garcia, J.L.; Mesa-Torres, N.; Neira, J.L.; Guzzi, R.; Pey, A.L. Phosphorylation compromises FAD binding and intracellular stability of wild-type and cancer-associated NQO1: Insights into flavo-proteome stability. *Int J Biol Macromol* 2019, *125*, 1275-1288.

31. Mesa-Torres, N.; Betancor-Fernández, I.; Oppici, E.; Cellini, B.; Salido, E.; Pey, A.L. Evolutionary Divergent Suppressor Mutations in Conformational Diseases. *Genes* 2018, *9*, E352.

32. Medina-Carmona, E.; Betancor-Fernández, I.; Santos, J.; Mesa-Torres, N.; Grottelli, S.; Batlle, C.; Naganathan, A.N.; Oppici, O.; Cellini, B.; Ventura, S.; Salido, E.; Pey, A.L. Insight into the specificity and severity of pathogenic mechanisms associated with missense mutations through experimental and structural perturbation analyses. *Human Molecular Genetics* 2019, *28*, 1-15.

33. Pey, A.L. Biophysical and functional perturbation analyses at cancer-associated P187 and K240 sites of the multifunctional NADP(H):quinone oxidoreductase 1. *Int J Biol Macromol* 2018, *118*, 1912-1923.

34. Munoz, I.G.; Morel, B.; Medina-Carmona, E.; Pey, A.L. A mechanism for cancer-associated inactivation of NQO1 due to P187S and its reactivation by the consensus mutation H80R. *FEBS Lett* 2017, *591*, 2826-2835.

35. Lienhart, W.D.; Strandback, E.; Gudipati, V.; Koch, K.; Binter, A.; Uhl, M.K.; Rantasa, D.M.; Bourgeois, B.; Madl, T.; Zangger, K.; Gruber, K.; Macheroux, P. Catalytic competence, structure and stability of the cancer-associated R139W variant of the human NAD(P)H:quinone oxidoreductase 1 (NQO1). *FEBS J* 2017, *284*, 1233-1245.

36. Medina-Carmona, E.; Fuchs, J.E.; Gavira, J.A.; Mesa-Torres, N.; Neira, J.L.; Salido, E.; Palomino-Morales, R.; Burgos, M.; Timson, D.J.; Pey, A.L. Enhanced vulnerability of human proteins towards disease-associated inactivation through divergent evolution. *Human Molecular Genetics* 2017, *26*, 3531-3544.

37. Zhang, Z.; Smith, D.L. Determination of amide hydrogen exchange by mass spectrometry: a new tool for protein structure elucidation. *Protein Sci* 1993, *2*, 522-531.

38. Trcka, F.; Durech, M.; Vankova, P.; Chmelik, J.; Martinkova, V.; Hausner, J.; Kadek, A.; Marcoux, J.; Klumpler, T.; Vojtesek, B.; Muller, P.; Man, P. Human Stress-inducible Hsp70 Has a High Propensity to Form ATP-dependent Antiparallel Dimers That Are Differentially Regulated by Cochaperone Binding. *Mol Cell Proteomics* 2019, *18*, 320-337.

39. Bai, Y. Hydrogen exchange experiments: detection and characterization of protein folding intermediates. In *Protein folding, misfolding and aggregation*; Muñoz, V., Ed. Royal Society of Chemistry: Cambridge, UK., 2008; pp. 70-83.

40. Konermann, L.; Pan, J.; Liu, Y.H. Hydrogen exchange mass spectrometry for studying protein structure and dynamics. *Chem Soc Rev* 2011, *40*, 1224-1234.

41. Megarity, C.F.; Abdel-Bettley, H.; Caraher, M.C.; Scott , K.A.; RA, W.; Jowitt, T.A.; Gutierrez, A.; Bryce, R.A.; Nolan, K.A.; Stratford, I.J.; Timson, D.J. Negative cooperativity in NADP(H) quinone oxidoreductase 1 (NQO1). *ChemBioChem* 2019. doi: 10.1002/cbic.201900313.

42. Wyman, J.; Gill, S.J. *Binding and Linkage. Functional Chemistry of Biological Macromolecules*; University Science Books: Mill Valley, 1990.